1-10-1995

The Origin of N III λ990 and C III λ977 Emission in AGN Narrow-Line Region Gas

Jason W. Ferguson
University of Kentucky

Gary J. Ferland
University of Kentucky, gary@uky.edu

A. K. Pradham
Ohio State University

The Origin of N III λ990 and C III λ977 Emission in AGN Narrow-Line Region Gas

Notes/Citation Information
Published in *The Astrophysical Journal Letters*, v. 438, no. 2, p. L55-L58.

Digital Object Identifier (DOI)
http://dx.doi.org/10.1086/187714

THE ASTROPHYSICAL JOURNAL, 438:L55–L58, 1995 January 10

THE ORIGIN OF N III λ990 AND C III λ977 EMISSION IN AGN NARROW-LINE REGION GAS

J. W. FERGUSON,[1] G. J. FERLAND,[1] AND A. K. PRADHAN[2]
Received 1994 August 8; accepted 1994 October 21

ABSTRACT

We discuss implications of HUT detections of C III λ977 and N III λ990 emission from the narrow-line region of the Seyfert 2 galaxy NGC 1068. In their discovery paper Kriss et al. showed that the unexpectedly great strength of these lines implies that the emitting gas must be shock-heated if the lines are collisionally excited. Here we investigate other processes which excite these lines in photoionization equilibrium. Recombination, mainly dielectronic, and continuum fluorescence are strong contributors to the line. The resulting intensities are sensitive to the velocity field of the emitting gas and require that the turbulence be of the same order of magnitude as the observed line width. We propose optical observations that will decide whether the gas is collisionally or radiatively heated.

Subject headings: galaxies: individual (NGC 1068) — galaxies: Seyfert — ISM: atoms — line: formation — quasars: emission lines

1. INTRODUCTION

Emission-line regions of active galactic nuclei (AGNs) probe fundamental questions about the nature of AGNs. Spectra of the broad- and narrow-line regions (BLRs and NLRs, respectively) offers clues to the chemical composition of the gas and the origin of the AGN luminosity, questions fundamental to the chemical evolution of galaxies and the nature of the activity. The energy source for the emission-line regions is one of the most fundamental, since this is pivotal in calibrating the lines as luminosity or composition indicators.

We investigate the origin of the N III λ990 and C III λ977 lines discovered by the Hopkins Ultraviolet Telescope (HUT) in the spectrum of NGC 1068 (Kriss et al. 1992). Kriss et al. showed that the lines are unexpectedly strong and cannot be attributed to collisional excitation by a photoionized gas. Collisional excitation in a shock-heated gas is one way to account for the observed intensity. Here we show that dielectronic recombination and continuum fluorescent excitation come into play in a photoionized gas, and that the observations are consistent with photoionization, and probe the velocity field of the emitting region.

2. THE OBSERVATIONAL CONUNDRUM

We summarize the NLR spectrum of NGC 1068 and its reddening correction, and outline the problems posed by the intensities of the emission lines λλ977, 990. We combined data from several sources to produce an observed UV-optical emission-line spectrum (Table 1). For $\lambda < 1800$ Å we use the HUT data of Kriss et al., and for λ longward of 1800 Å we use the data from Snijders, Netzer, & Boksenberg (1986).

Kriss et al. (1992) show that the NLR lines have varying widths, ranging from 1000 to 3200 km s^{-1}. The situation is likely to be analogous to that of other NLRs (Halpern & Filippenko 1984; Osterbrock & Veilleux 1987), with NLR emission arising from a variety of locations and conditions. Here we will focus on intermediate ionization species, C^{+2}, C^{+3}, N^{+2}, and N^{+3} and model the ratios N III λ990/N III] λ1750, N IV] λ1486/N III] λ1750, C III λ977/C III] λ1909, and C IV λ1549/C III] λ1909. These determine conditions for the emitting region, and have the advantage of being insensitive to the unknown composition of the gas. The line widths of the N III], N III, N IV], C III, and C IV line widths are within roughly 1 σ of one another (the C III] intensity is taken from Snijders et al. 1986, and a line width is not available). We do not attempt to model either high-ionization (i.e., O VI λ1034, N V λ1240, or the He II lines) or neutral molecular gas.

2.1. *The Reddening Problem*

He II is the most powerful reddening indicator present in our spectrum, because of its expected simplicity. Resonance lines ionize H^0 and He^0, and are destroyed before scattering often enough to create a substantial population in the $n = 2$ level. Because of this optical/UV lines remain optically thin for NLR conditions (MacAlpine 1981). The observed He II lines have very high excitation potentials (~50 eV), so collisional excitation should be inefficient. The observed He II spectrum should be close to case B (Seaton 1978).

We have two reddening indicators which sense different portions of the spectrum. The He II λ4686/λ1640 ratio is expected to be ~7.5, and the λ1640/λ1085 ratio is expected to be 6.6. As pointed out by Kriss et al. (1992), for ISM ($R = 3.1$) extinction (Cardelli, Clayton, & Mathis 1989), we find two different extinctions, $A_V = 0.95 \pm 0.05$ for the 4786–1640 Å range, and $A_V = 0.53 \pm 0.05$ for the 1640–1085 Å range. Either the He II spectrum is not well represented by case B, or the extinction curve for NGC 1068 is anomalous. The sense of the anomaly is that the extinction is "grayer" than expected for an $R = 3.1$ ISM curve in the 1085–1640 Å wavelength range. This type of gray UV extinction is observed in Orion, so, following Kriss et al., we adopt anomalous reddening as the likely culprit.

We use the $R = 3.1$ curve and correct the range between the optical and 1640 Å with $A_V = 0.95$, and wavelengths below 1640 Å with the same extinction curve but with $A_V = 0.53$. This is expected to be a safe assumption for the lines between these limits, since we are *interpolating* on reddening corrections which give the correct He II spectrum at either extreme. Unfortunately, it is necessary to *extrapolate* the extinction curve to the 980 Å region to include N III and C III lines.

We judge the uncertainty introduced by this extrapolation by comparing results from the standard ISM with results of

[1] Department of Physics and Astronomy, University of Kentucky, Lexington, KY 40506.
[2] Department of Astronomy, Ohio State University, Columbus, OH 43210.

TABLE 1

OBSERVED AND PREDICTED EMISSION-LINE SPECTRUM

Spectrum	λ(Å)	Observed[1]	Corrected[2]	Predicted[2,3]
CIII	977	7.6 ± 1.4	2.54 ± 0.79	2.07
Rec.	977			0.02
Coll.	977			0.15
Pump	977			1.90
NIII	990	3.9 ± 1.0	1.18 ± 0.42	1.22
Rec.	990			0.23
Coll.	990			0.72
Pump	990			0.27
HeII	1085	3.7 ± 1.0	0.68 ± 0.18	--
NIV	1486	5.1 ± 1.1	0.42 ± 0.09	0.37
CIV	1549	39.7 ± 3.0	3.16 ± 0.24	3.27
HeII	1640	21.4 ± 1.6	4.44 ± 0.33	--
NIII]	1750	5.7 ± 1.5	1.15 ± 0.30	0.98
CIII]	1909	24.0 ± 3.5	5.39 ± 0.79	5.67
HeII	4686	9.0 ± 2.0	0.59 ± -.13	--
Hβ	4861	16.0 ± 2.0	1.00 ± 0.13	1.00

[1] In units of ergs cm^{-2} s^{-1} Hz^{-1} at Earth.
[2] Relative to Hβ.
[3] Predicted by complete model as described in text.

Orion ($R = 5.3$) extinction. In the second case we derive $A_V = 3.70 \pm 0.05$ for the 4686–1640 Å range, and $A_V = 4.90 \pm 0.05$ for the 1640–1085 Å range. We find N III λ1990/λ1750 of 1.03 and 1.65, and C III λ977/λ1909 of 0.47 and 0.61 for the ISM and Orion extinction extrapolation, respectively. This uncertainty is approximately the same as the observational uncertainty.

Column (3) of Table 1 gives the reddening-corrected spectrum used in the following sections, adopting the $R = 3.1$ curve. The uncertainties for C III and N III have been increased to account for the uncertainty introduced by the reddening correction.

2.2. *Collisional* C III λ977/λ1909 *and* N III λ990/λ1750 *Ratios*

The C III λ977/C III] λ1909 and N III λ990/N III] λ1750 intensity ratios are simple functions of electron temperature if all lines are collisionally excited. If we assume that each collisional excitation results in one line photon, then

$$\left(\frac{977}{1909}\right) = \frac{1909}{977}\frac{q_{977}}{q_{1909}} = \frac{1909}{977}\frac{Y_{977}}{Y_{1909}}\exp\left(-\frac{\Delta\chi}{kT}\right)$$
$$\approx 8.0\exp\left(-\frac{71{,}800\ \mathrm{K}}{T}\right).$$

The q's represent collisional excitation rate coefficients, and the Y's are thermally averaged electron impact collision strengths (Berrington 1985a, b). For photoionization equilibrium $T \approx 10^4$ K, and the line ratio is less than 1%. The observed line ratio is 0.47, corresponding to $T \approx 25{,}400 \pm 7900$ K. For λ990/λ1750 (Blum & Pradhan 1992) we predict 1% for 10^4 K, and require $T \approx 35{,}800 \pm 12{,}700$ K to match the observed ratio of 1.03. These high temperatures are the basis for the conclusion that the clouds are shock-ionized.

3. N III λ990 AND C III λ977 IN PHOTOIONIZED NEBULAE

Here we show that other processes contribute to these lines.

3.1. *Dielectronic Recombination*

Effective recombination coefficients for both lines have been computed by Nussbaumer & Storey (1984). We adopt these values for the present work.

3.2. *Bowen Fluorescence*

Our treatment of this process is presented in Netzer, Elitzur, & Ferland (1985). This process only affects the N III line.

3.3. *Continuum Fluorescence*

Both lines can be excited by continuum fluorescence. We adopt the formalism outlined by Ferland (1992). The essential approximation is that once a line is excited following absorption of a continuum photon, it will scatter and be degraded into subordinate lines with probability given by the branching ratio. This is equivalent to the "case B" approximation for formation of hydrogen Lyman lines (Osterbrock 1989).

The radiative transition probabilities used here were obtained from the Opacity Project database (Cunto et al. 1993). The Be-sequence data, e.g., for C III, were calculated by Tully, Seaton, & Berrington (1990), and the B-sequence data, e.g., N III, by Fernley et al. (1994). All C III excitations will eventually result in a λ977 photon. The six driving transitions that we include are the $2s^2$ ground term to $2s2p$, $2s3p$, $2s4p$, ..., $2s8p$. The driving transitions for N III are the $2s^22p$ ground term to $2s^23d$, $2s^24s$, $2s2p3p$, $2s^24d$. Grotrian diagrams for C III and N III can be found in Bashkin & Stoner (1975).

With these assumptions, the number of line photons produced by continuum fluorescence is proportional to the continuum intensity at the wavelength of the driver lines and the line width, if the line is optically thick. The line width entering the line optical depth scale is given by

$$v^2_{\mathrm{Doppler}} = 2kT/m + v^2_{\mathrm{turb}},$$

where m is the atom's mass and the last term is the turbulent velocity.

For the case where there are n resonance lines in the neighborhood of wavelength λ, the intensity of C III λ977 relative to Hβ is given by

$$\frac{977}{\mathrm{H}\beta} = \frac{4861}{977}\frac{n v_{\mathrm{Doppler}}\,\varphi_v(\lambda)}{Q(\mathrm{H})}\frac{\alpha_B}{\alpha_{\mathrm{eff}}(\mathrm{H}\beta)}$$
$$\approx 1.20\left(\frac{n}{6}\right)\left(\frac{v_{\mathrm{Doppler}}}{1000\ \mathrm{km\ s^{-1}}}\right),$$

where the α's are the Hβ effective and hydrogen case B recombination coefficients (Osterbrock 1989), $\phi_v(\lambda)$ is the continuum flux density per unit velocity (photons cm^{-3}), and $Q(\mathrm{H})$ is the integrated flux of hydrogen ionizing photons (photons cm^{-2} s^{-1}). We use the NGC 1068 continuum shape deduced by Marshall et al. (1993). There is no explicit dependence on the carbon abundance, other than that implicit in the assumption that the lines are optically thick. For the assumed parameters (six driving lines and a Doppler width of 1000 km s^{-1}) the predicted line ratio is roughly half of the observed value.

3.4. *Computational Details*

The code described by Ferland (1993) has been modified to include continuum fluorescent excitation for all lines which can become optically thick. The fluorescent probability (Ferland 1992) is integrated over the structure and included as an additional excitation mechanism. In this formalism turbulent line width only enters by modifying the optical depth scale.

Continuum excitation can be an efficient heating mechanism for the cloud (Tielens & Hollenbach 1985). This is treated by writing, the line cooling as $(n_l q - n_u q_{ul})h\nu$, while the line inten-

sity is $n_u A_{ul} h\nu$. The u and l indicate the upper and lower levels of the transition.

All of the calculations in this paper include grains. Line destruction by background opacity is treated using the formalism of Hummer (1968) and Elitzur & Netzer (1985). This destruction probability depends on the ratio of the line-center opacity to the background opacity, introducing another dependence on the turbulence (the line-center opacity decreases with line width).

3.5. *Illustrative Calculations*

We assume constant cloud density and solar abundances, with ISM grains (Baldwin et al. 1991) and gas-phase depletions. The abundances used were H:He:C:N:O:Ne:Na:Mg:Al:Si:S:Cl:Ar:Ca:Fe:Co:Ni = 100,000:9500:16.25:11.37:21.66:5.96:0.016:1.63:0.011:0.163:0.54:0.006:0.163:0.001:0.163:0.00005:0.00098.

Figure 1 shows the results of a series of calculations in which the hydrogen density was held fixed at $n_H = 10^{5.5}$ cm^{-3}, and the ionization parameter U, the dimensionless ratio of densities of ionizing photons to free electrons, is varied. The turbulent line width is also varied, with values of 0, 100, and 1000 km s^{-1} plotted.

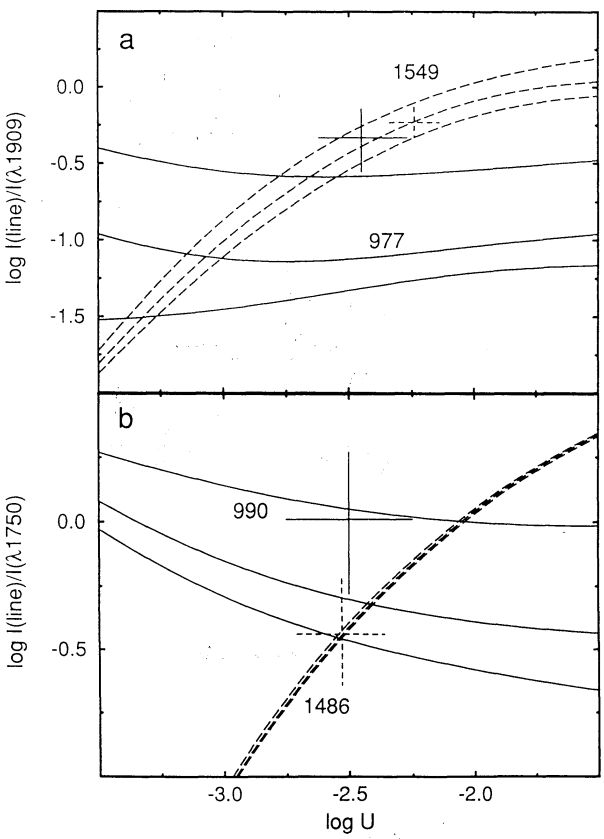

FIG. 1.—C and N spectra as functions of ionization parameter U and turbulent velocity. (*a*) Solid lines represent C III/C III], and dashed curves represent C IV/C III], for the turbulent velocities of 0, 100, and 1000 km s^{-1} listed from the bottom upward for each line ratio. (*b*) Similar to (*a*), the solid curves being for N III/N III] and the dashed curves for N IV/N III]. The crosses in each diagram represent the observed ratios (*vertical bars*) and the estimated uncertainty in the ionization parameter (*horizontal bars*); the solid cross represents C III/C III] in (*a*) and N III/N III] in (*b*), and the dashed cross is C IV/C III] in (*a*) and N IV/N III] in (*b*).

The C IV/C III] ratio is mainly sensitive to the ionization parameter (Davidson & Netzer 1979). C III] is not affected by fluorescence, since it is optically thin here. C IV is optically thick and has a significant fluorescent component for large turbulence, mainly from reflected continuum radiation. The C III/C III] ratio is sensitive to turbulence because the C III line is strengthened by fluorescence, unlike the C III] line. Similar arguments hold for the nitrogen spectrum, although here the N III] and N IV] lines are optically thin and unaffected by turbulence.

We see that the entire C III, C III], C IV, N III], N III, and N IV spectrum can be roughly explained for an ionization parameter of $-2.6 \leq \log U \leq -2.3$ and 500 km s^{-1} $\leq v_{turb} \leq$ 2000 km s^{-1}.

3.6. *A Complete Model*

We optimize a full model by varying several parameters, including the turbulent velocity, ionization parameter, and overall metallicity of the gas. We allow the grains and metals to vary together, with a constant ratio, essentially assuming that the dust-to-gas ratio scales linearly with metallicity. For simplicity we do not investigate other continuum shapes.

We attempt to model only the intermediate ionization region. Regions with extremes of ionization must also be present. A complete model of the NLR must integrate over a population of clouds with different physical conditions (Halpern & Filippenko 1984).

The optimization uses a χ^2 minimization to match the observed and predicted intensities. The best-fitting parameters were $\log U = -2.53$, $v_{turb} = 2000$ km s^{-1}, with the metallicity and grain abundance at 0.72 times solar. The resulting spectrum is given in Table 1.

The results of this modeling approach are not unique. Other continuum shapes, or a different treatment of the reddening, may well have led to other deduced quantities. (Tests show that the deduced parameters are sensitive to the unknown form of the reddening curve below 1085 Å.) The good fit shows that photoionization alone can account for the observed spectrum.

4. DISCUSSION

We have presented a general theory of the formation of the C III and N III extreme ultraviolet lines for low-density gas. The turbulence is introduced as a free parameter. Continuum fluorescence is an important excitation mechanism for larger values of the turbulent velocity field. The observed spectrum of NGC 1068 can easily be reproduced by photoionization equilibrium if the gas is highly turbulent, without recourse to alternative energy sources such as shock heating.

The introduction of line width as a free parameter introduces the question of the nature of the observed line width of NLR gas (Whittle 1993). Rotation of the host galaxy or bulk motions of coherent objects would result in only a thermal line width over the line of sight through a cloud to the continuum source. The theory we outline here requires that the line broadening exist across the line-forming region. The microturbulent line broadening we require would be more appropriate for a wind or chaotic motions.

This does not demonstrate that NLR gas must be photoionized. An observational test to determine whether the N III λ990 line is predominantly collisionally excited (which would require shock heating), or has a strong contribution from fluorescence and recombination as we argue, is possible. Figure 1

of Netzer et al. (1985) shows that the N III λ4640 multiplet is also produced by the "extra" processes we describe. Pure fluorescent excitation results in a λ4640/λ990 ratio which is only a function of branching ratios. The theoretical value is λ4740/λ990 ≈ 17.6%. High signal-to-noise optical observations of NGC 1068, and suitable limits or detection of λ4640, can determine whether the NLR is shock-ionized or photoionized.

We thank the NSF for support through grants AST 93-19034 and PHY-9115057, and NASA for support through grant NAGW-3315.

REFERENCES

Baldwin, J., Ferland, G. J., Martin, P. G., Corbin, M., Cota, S., Peterson, B. M., & Slettebak, A. 1991, ApJ, 374, 580
Bashkin, S., & Stoner, J. O. 1975, Atomic Energy Levels and Grotrian Diagrams, Vol. 1 (Amsterdam: North-Holland)
Berrington, K. A. 1985a, J. Phys. B, 18, L395
———. 1985b, Atomic Data Nucl. Data Tables, 33, 195
Blum, R. D., & Prahan, A. K. 1992, ApJS, 80, 425
Cardelli, J. A., Clayton, G. C., & Mathis, J. S. 1989, ApJ, 345, 245
Cunto, W., Mendoza, C., Ochsenbein, F., & Zeippen, C. J. 1993, A&A, 275, L5
Davidson, K., & Netzer, H. 1979, Rep. Prog. Phys., 51, 715
Elitzur, M., & Netzer, H. 1985, ApJ, 291, 464
Ferland, G. J. 1992, ApJ, 389, L63; erratum 434, L37 (1994)
———. 1993, Univ. Kentucky Dept. Physics and Astron. Internal Rept.
Fernley, J. A., Hibbert, A., Kingston, A. E., & Seaton, M. J. 1994, private communication
Halpern, J. P., & Filippenko, A. V. 1984, ApJ, 285, 475
Hummer, D. G. 1968, ApJ, 138, 73
Kriss, G. A., Davidson, A. F., Blair, W. P., Ferguson, H. C., & Long, K. S. 1992, ApJ, 394, L37
MacAlpine, G. M. 1981, ApJ, 251, 465
Marshall, F. E., et al. 1993, ApJ, 405, 168
Netzer, H., Elitzur, M., & Ferland, G. J. 1985, ApJ, 299, 752
Nussbaumer, H., & Storey, P. J. 1984, A&AS, 56, 293
Osterbrock, D. E. 1989, Astrophysics of Gaseous Nebulae and Active Galactic Nuclei (Mill Valley: University Science Books)
Osterbrock, D. E., & Veilleux, S. 1987, ApJS, 63, 295
Seaton, M. J. 1978, MNRAS, 185, 5P
Snijders, M. A. J., Netzer, H., & Boksenberg, A. 1986, MNRAS, 222, 549
Tielens, A. G. G. M., & Hollenbach, D. 1985, ApJ, 291, 722
Tully, J. A., Seaton, M. J., & Berrington, K. A. 1990, J. Phys. B, 23, 3811
Whittle, M. 1993, in The Nearest Active Galaxies, ed. J. Beckman, L. Colina, & H. Netzer (Dordrecht: Kluwer), 17